Journal of Power Sources 195 (2010) 2003–2007

Contents lists available at ScienceDirect

Journal of Power Sources

journal homepage: www.elsevier.com/locate/jpowsour

Short communication

Hydrogen storage behaviour of Li_3N doped with Li_2O and Na_2O

Henrietta W. Langmi*, Scott D. Culligan, G. Sean McGrady*

Department of Chemistry, University of New Brunswick, 30 Dineen Drive, Fredericton, N.B. E3B 5A3, Canada

ARTICLE INFO

Article history:
Received 14 September 2009
Accepted 4 October 2009
Available online 12 October 2009

Keywords:
Hydrogen storage
Lithium nitride
Lithium oxide
Sodium oxide

ABSTRACT

Mixtures of Li_2O/Li_3N and Na_2O/Li_3N have been investigated for hydrogen storage. When Li_3N is doped with *ca.* 5 mol% Li_2O and annealed, both binary compounds exist as separate phases as evident from powder X-ray diffraction. Li_2O acts as a spectator in the hydrogen storage reactions and there is no evidence of enhanced Li^+ or H^+ mobility. Na_2O (5 mol%) interacts more strongly with Li_3N, leading to the generation of an unidentified phase, which also appears to play no part in the hydrogen storage reactions of the composite system. We conclude that addition of these levels of Li_2O or Na_2O to Li_3N followed by annealing does not improve the hydrogen storage properties of Li_3N.

1. Introduction

There are increasing concerns about the environmental pollution caused by carbon-based fuels, and the depletion of natural reservoirs of these fuels. Hydrogen is an ideal alternative to fossil fuels. However, one of the main challenges concerning the use of hydrogen is the development of a suitable storage medium [1]. Solid-state hydrogen storage materials allow hydrogen to be stored in a compact and safe manner. Many research efforts are focused on solid-state materials such as light metal hydrides and their complexes [2]. Lithium nitride has recently emerged as a promising material for hydrogen storage [3]. It has a theoretical hydrogen storage capacity of 11.5 wt.%, and undergoes hydrogenation/dehydrogenation in two main steps [3,4]:

$$Li_3N + H_2 \leftrightarrow Li_2NH + LiH \qquad \Delta H = -116\,kJ\,mol^{-1} \tag{1}$$

$$Li_2NH + H_2 \leftrightarrow LiNH_2 + LiH \qquad \Delta H = -45\,kJ\,mol^{-1} \tag{2}$$

Although in practice, 9.3 wt.% hydrogen is attainable above 250 °C, complete desorption is achieved only at temperatures above 320 °C in dynamic vacuum [3]. In fact, the effective reversible hydrogen storage capacity of Li_3N is about 5.5 wt.% at 280 °C or lower [5]. Accordingly, reaction (1) has a much larger negative enthalpy than reaction (2) accounting for the partial desorption of hydrogen under milder conditions.

Considerable research effort has focused on enhancing the hydrogen storage characteristics of the Li–N–H system. For example, addition of catalytic amounts of transition metals or metal chlorides [6,7] and partial substitution of Li with Mg [8,9] has been shown to enhance its performance. Furthermore, there has been increasing interest in amide–hydride mixtures, particularly those involving $Mg(NH_2)_2/LiH$, $LiNH_2/MgH_2$, $LiNH_2/LiBH_4$ and $LiNH_2/LiAlH_4$ [10–13]. Lithium nitride has an extremely high Li^+ ion conductivity ($\sim 10^{-4}\,\Omega^{-1}\,cm^{-1}$) and could potentially be used in lithium ion batteries [14]. In a recent study, David et al. [15] reported that for the Li–N–H system $LiNH_2/Li_2NH$ transformation is a bulk reversible reaction that occurs through a non-stoichiometric process, and proposed an ion migration mechanism involving Li^+ and H^+ ions. It was concluded that Li^+ mobility plays a key role in the hydrogenation/dehydrogenation reactions of Li_3N.

In the light of the ion migration mechanism proposed by David et al., we have prepared mixtures of Li_3N incorporating small amounts of Li_2O. An earlier study demonstrated that Li_3N, partially oxidized by exposure to air followed by heat treatment in vacuo, exhibits improved hydrogen storage properties [16]. In the current work, doping of Li_3N with Li_2O was carried out in an attempt to introduce cation vacancies that may assist Li^+ mobility. By using Li_2O as our dopant, aliovalent substitution of N^{3-} in Li_3N by O^{2-} should occur, creating Li^+ vacancies to compensate for the charge imbalance, which should increase Li^+ mobility [17]. Aliovalent substitution of N^{3-} in Li_3N by NH^{2-} has been reported [18]. In the hydrogenated products of Li_3N (i.e. $LiNH_2$ and LiH), the presence of many mobile Li^+ ions implies increased likelihood of creating more H^+ ions (according to the ion migration model), which should have an impact on the hydrogen storage properties of the Li–O–N–H system. As a follow up to this study, we have prepared analogous mixtures of Li_3N and Na_2O. Na_2O has itself been reported to reversibly absorb hydrogen, forming NaH and NaOH [19]. To the best of our knowledge, no studies of a composite Na_2O/Li_3N system for hydrogen

* Corresponding authors. Tel.: +1 506 452 6340; fax: +1 506 453 4981.
E-mail addresses: hlangmi@unb.ca (H.W. Langmi), smcgrady@unb.ca (G.S. McGrady).

0378-7753/$ – see front matter © 2009 Elsevier B.V. All rights reserved.
doi:10.1016/j.jpowsour.2009.10.008

storage have been previously reported. Here we report for the first time an investigation of Na_2O-doped Li_3N for hydrogen storage.

2. Experimental

2.1. Synthesis and manipulation

Commercial powders of Li_3N (STREM, 99.5%), Li_2O (Aldrich, 97%, 60 mesh) and Na_2O (Aldrich, 80%) were used as starting materials. All material and sample manipulations were carried out in a nitrogen-filled glovebox to minimize contamination with atmospheric oxygen and moisture. In the first study Li_3N was mixed with 2 and 5 mol% Li_2O. In the second study it was mixed with 5 mol% Na_2O. The total mass of each mixture was 10 g. These samples were loaded in a 250 mL stainless steel milling vessel containing five stainless steel balls with a diameter of 20 mm, then milled using a Retsch PM100 planetary mill. The ball-to-powder mass ratio was 16:1. Milling was carried out for 3 h at room temperature in a N_2 atmosphere at a rotational speed of 200 rpm. In order to minimize the temperature increase due to milling, the parameters of the mill were set such that after every 5 min of milling in one direction the mill paused for 10 s and then rotated in the reverse direction. The milled sample was then annealed at high temperature. In this procedure, 1.2 g of sample was placed in a monel crucible and loaded in a custom-made quartz tube inside a nitrogen-filled glovebox. The tube was then inserted into a tube furnace and was maintained at either 400 or 620 °C under a flowing stream of nitrogen gas for 12 h. In addition to the doped materials unmilled and milled Li_3N (both undoped) were also investigated in this study.

2.2. Characterization of materials

Samples were characterized by powder X-ray diffraction (XRD), using a Bruker D8 Advance diffractometer or Rigaku Miniflex diffractometer both equipped with a Cu Kα radiation source. Product identification was carried out by reference to the Joint Committee for Powder Diffraction Studies (JCPDS) values in the database of the diffractometer. During XRD analysis, parafilm was used to cover the samples to prevent contact with air during the measurement. Diffraction peaks at *ca.* 21.6° and 24° arising from parafilm were observed in all the XRD patterns. Differential Scanning Calorimetry (DSC) measurements were performed using a TA Instruments Q20P DSC. In a typical experiment with unhydrogenated samples, 9–10 mg of material was used and the DSC cell was pressurized to an initial pressure of 30 bar with H_2 gas. The sample was heated to 500 °C at 5 °C min^{-1}. Hydrogen absorption/desorption performance was examined using a commercial PCTPro-2000 Sieverts-type instrument manufactured by HyEnergy LLC. High purity hydrogen (Air Liquide, 99.999%) was used in all experiments. For absorption experiments, initial pressure of 30 bar H_2 was employed. For both absorption and desorption, approximately 0.5 g of material was used; this was heated at 2 °C min^{-1} to the desired measurement temperature, where it was held for 12 h. Kinetic curves for both absorption and desorption were obtained. The hydrogen storage capacities reported are expressed as a wt.% of the entire sample.

3. Results and discussion

3.1. Li_2O-doped Li_3N

Fig. 1 shows the XRD patterns for Li_3N doped with 5 mol% Li_2O. This reveals both materials still to be present as the binary compounds, with no evidence of new peaks corresponding to a mixed Li–N–O phase. The unannealed sample showed the co-existence

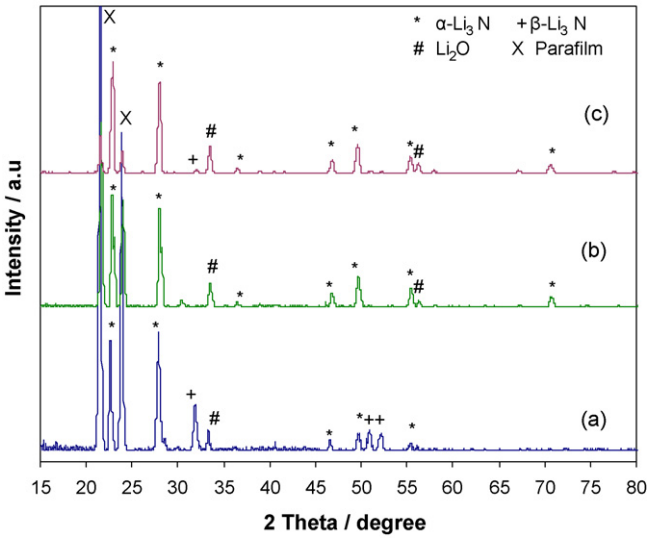

Fig. 1. XRD patterns for 5 mol% Li_2O-doped Li_3N: (a) no heat treatment, (b) annealed at 400 °C, and (c) annealed at 620 °C.

of both α- and β-Li_3N, as well as Li_2O (commercial Li_3N contains both α- and β-phases). After annealing at 400 °C, β-Li_3N was completely transformed to α-Li_3N according to the XRD pattern, which now indicated only α-Li_3N and Li_2O. This is consistent with a literature report that the transformation from β- to α-Li_3N occurs above 200 °C [20]. After heat treatment at 620 °C, the sample was composed predominantly of α-Li_3N and Li_2O, with possibly traces of β-Li_3N. For all three samples, it cannot be ruled out that some substitution of N^{3-} by O^{2-} had occurred, though the presence of remaining Li_2O was clearly evident in the XRD pattern in each case.

DSC experiments in hydrogen showed the profile for Li_2O to be essentially a flat line, indicating as expected that Li_2O did not absorb any hydrogen (Fig. 2). On the other hand, the curve for as-received Li_3N showed both exothermic and endothermic events. The onset of the exothermic event occurred at about 200 °C. This feature is broad, and as the temperature approached 330 °C a second exothermic peak was clearly seen. Both exothermic events are attributed to hydrogen absorption. We note that when the DSC experiments were carried out in nitrogen no thermal events were observed. As described in Eqs. (1) and (2), hydrogenation occurs in

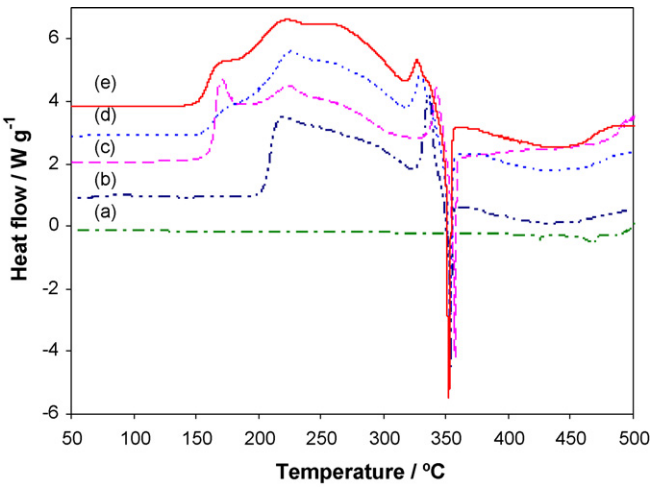

Fig. 2. DSC plots of hydrogen absorption by (a) Li_2O, (b) as-received Li_3N, (c) undoped (milled) Li_3N, (d) Li_3N doped with 2 mol% Li_2O (milled), and (e) Li_3N doped with 5 mol% Li_2O (milled).

two principal steps. The hydrogenated phases from the reactions are Li_2NH, LiH and $LiNH_2$. Accordingly, we assign the first event as the transformation of Li_3N to Li_2NH and LiH. As time progressed and the temperature increased, $LiNH_2$ was also generated. As the temperature approached 345 °C the formation of $LiNH_2$ accelerated, resulting in the second exothermic peak. Chien et al. [21] studied the evolution of Li_2ND, LiD and $LiND_2$ phases during hydriding of Li_3N by in situ neutron diffraction. For the isothermal transformation at 200 °C, these authors reported that the evolution of the hydrided phases was time dependent; transformation to Li_2ND and LiD occurred initially, and then rapid formation of $LiND_2$ began to occur concurrently.

It can also be seen from Fig. 2 that when Li_3N was milled without any dopant, the onset of the broad exothermic peak was at least 50 °C lower than that of as-received Li_3N. This was also the case when Li_3N was doped with 5 mol% Li_2O. Milling results in smaller particles implying enhanced sorption kinetics. Therefore, doping of Li_3N with 5 mol% Li_2O (without any heat treatment) has no significant effect on the onset temperature of hydrogen uptake. Presumably no additional Li^+ vacancies are created that would favour Li^+ and H^+ migration. Nevertheless, comparing the DSC data for the 5 mol% Li_2O-doped Li_3N and the 2 mol% Li_2O-doped Li_3N reveals that the latter had a relatively higher onset temperature. By comparison with as-received Li_3N these exothermic events are attributed to the formation of the hydrogenated phases of Li_3N. The sharp endothermic peak observed between 352 and 358 °C for as-received, undoped and doped Li_3N is associated with the melting of $LiNH_2$. Pure $LiNH_2$ melts at about 380 °C [22]. In the composite $LiNH_2$/LiH, the melting transition of $LiNH_2$ apparently occurs about 25 °C lower. After the endothermic peak a shift in the baseline occurred, which is consistent with a change in the specific heat of the sample in the liquid phase.

When Li_3N doped with 5 mol% Li_2O was annealed at 400 °C, the broad exothermic peak shifted to a higher temperature (Fig. 3), whose onset temperature is 215 °C compared to 150 °C for the sample before annealing. Annealing may result in larger particles and hence slower kinetics sorption. The endothermic peak associated with the melting of $LiNH_2$ was also apparent. However, once again it appears that there was no enhancement of Li^+ and H^+ mobility, implying that the postulated aliovalent substitution of N^{3-} in Li_3N by O^{2-} did not occur. When annealing was conducted at 620 °C, a subsequent increase in the onset temperature for the exothermic reaction was observed. After annealing at 620 °C the sample became a solid agglomerate that required crushing with a mortar and pestle in order to carry out further analysis. Such sintering may lead to an increase in the sizes of the particles. Remarkably, a very strong exothermic peak was clearly visible just before the endothermic melting peak of $LiNH_2$. The sharpness of this peak seems to suggest that while the transformation of Li_3N to Li_2NH was gradual the conversion of Li_3N and/or Li_2NH to $LiNH_2$ occurred quite rapidly.

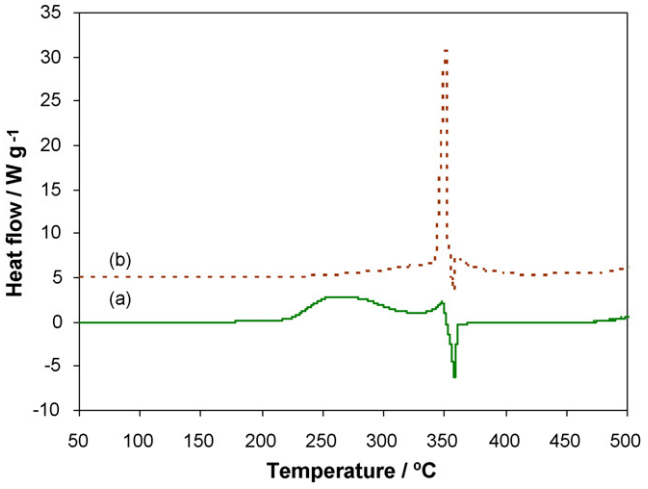

Fig. 3. DSC plots of hydrogen absorption by annealed 5 mol% Li_2O-doped Li_3N: (a) annealed at 400 °C and (b) annealed at 620 °C.

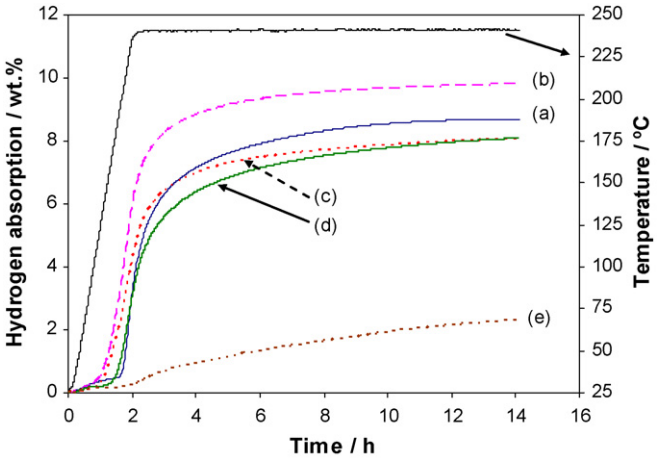

Fig. 4. Hydrogen absorption kinetic curves (room temperature to 240 °C) for (a) as-received Li_3N, (b) undoped (milled) Li_3N, (c) Li_3N doped with 5 mol% Li_2O (milled), (d) Li_3N doped with 5 mol% Li_2O (milled and annealed at 400 °C), and (e) Li_3N doped with 5 mol% Li_2O (milled and annealed at 620 °C).

Based on the DSC results, significant hydrogen uptake should occur at about 230–250 °C for almost all samples, as part of the broad exothermic peak falls within this region in most cases. Accordingly, sequential hydrogen absorption–desorption measurements were carried out at 240 °C for all samples. The hydrogen absorption curves at 240 °C are shown in Fig. 4. It can be seen that while as-received, undoped, doped Li_3N and doped Li_3N annealed at 400 °C absorbed considerable amounts of hydrogen (>8 wt.%), the hydrogen uptake capacity of doped Li_3N annealed at 620 °C reached only 2.3 wt.% under the same conditions. Fig. 4 clearly reveals that significant hydrogen absorption occurred at a relatively lower temperature for the milled undoped and doped samples than for the other materials, in line with the DSC data discussed above. Evidently, the undoped sample demonstrated highest hydrogen absorption capacity at 240 °C. Though the unannealed doped sample showed relatively higher hydrogen storage capacity at lower temperatures than the other materials, its hydrogen storage capacity reached the same value as the doped sample annealed at 400 °C. Thus, heat treatment apparently had an effect on the doped sample pushing the onset of hydrogenation to higher temperature. This effect is enhanced at a higher temperature, as demonstrated by the sample that was annealed at 620 °C; very little hydrogen uptake was achieved at 240 °C. However, at 345 °C up to 9.1 wt.% hydrogen uptake was attained in the latter sample although less than 4 wt.% hydrogen could be desorbed at same temperature within the time frame of the experiment (Fig. 5). This high hydrogen uptake observed here is in good agreement with the strong exothermic peak observed in the DSC experiments (Fig. 3). The hydrogenated samples were characterized by powder XRD. Hydrogenation was incomplete, as some Li_3N could still be detected in the XRD pattern. The hydrogenated products were $LiNH_2$ and LiH, in line with the conclusion drawn from the DSC results. In addition, Li_2O was also present. Therefore, the hydrogenation reaction is essentially the same as that for Li_3N, with Li_2O being a spectator in the reaction.

Hydrogen desorption commenced at about the same temperature (~220 °C) for all samples. As expected, the least amount of hydrogen desorption was observed for the sample that was annealed at 620 °C. Hydrogen desorption from the as-received and

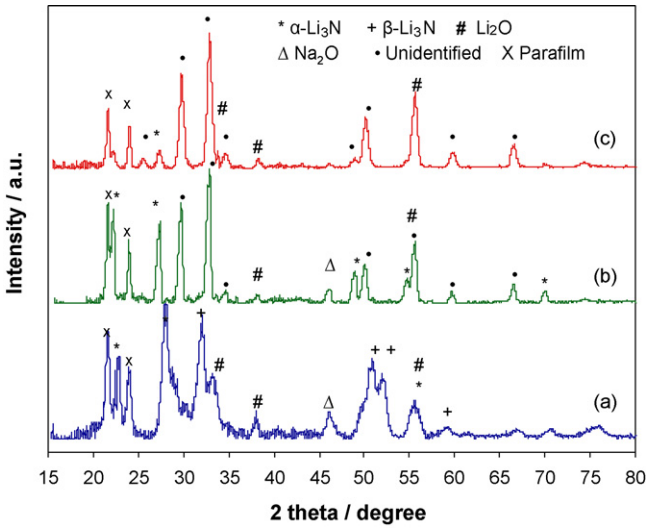

Fig. 5. XRD patterns for 5 mol% Na_2O-doped Li_3N: (a) no heat treatment, (b) annealed at 400 °C, and (c) annealed at 620 °C.

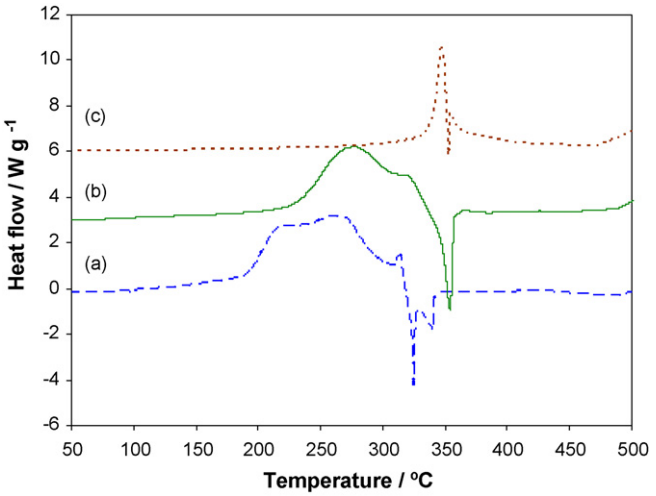

Fig. 6. DSC plots of hydrogen absorption by 5 mol% Na_2O-doped Li_3N: (a) unannealed (milled), (b) annealed at 400 °C, and (c) annealed at 620 °C.

doped Li_3N was quite similar, reaching about 1.6 wt.% after 12 h at 240 °C. The highest amount of hydrogen desorption (2.7 wt.%) was achieved by the undoped sample. Hydrogen desorption from the doped sample that was annealed at 400 °C was also considerable, reaching 2.5 wt.%. Giving that the hydrogen storage capacities are expressed as a wt.% of the total material, the values for these latter two samples are comparable when expressed as wt.% of Li_3N alone. After this initial desorption experiment, a second absorption experiment was performed under the same conditions. It was noted that the sample that was annealed at 400 °C reabsorbed the most hydrogen (3.2 wt.%). The undoped milled material also reabsorbed a substantial amount of hydrogen (3.0 wt.%). Therefore, doping with Li_2O followed by annealing at 400 °C had only a slight effect on the hydrogen reabsorption capacity of Li_3N.

3.2. *Na_2O-doped Li_3N*

Powder XRD patterns for Li_3N doped with 5 mol% Na_2O are presented in Fig. 5. Before annealing, α-Li_3N, β-Li_3N, Na_2O, and possibly Li_2O, co-existed in the sample. Similarly to Li_2O-doped Li_3N, it appears that upon annealing β-Li_3N transformed to α-Li_3N, but with a slight shift of the α-Li_3N reflections to lower 2θ values. Many strong unidentified diffraction peaks also emerged after annealing. At first glance some of these peaks appeared to belong to β-Li_3N but with a shift in 2θ values. However, this material was annealed at high temperatures (400 and 620 °C), at which β-Li_3N is expected to transform to α-Li_3N [20], as was observed for the Li_2O/Li_3N system. These diffraction peaks persisted after hydrogenation (*q.v.*), implying that they do not correspond to β-Li_3N. They also cannot be assigned to any of the compounds found in the JCPDS database; specifically, the peaks cannot be assigned to a peroxide, nitrite, nitrate, other oxynitride or azide salt of lithium or sodium. We are currently exploring the identity and nature of this phase, although it appears to play no role in the hydrogen storage properties of the system.

Fig. 6 shows the DSC characteristics of the doped sample to be different from that of the as-received sample (cf. Fig. 2). The broad exothermic event that began at about 195 °C is attributed to hydrogen absorption. Two endothermic peaks also occurred at *ca.* 325 and 340 °C. These are probably melting transitions, most likely of NaOH and $LiNH_2$, respectively. We note that the melting points of pure NaOH and $LiNH_2$ are 318 and 380 °C, respectively. As mentioned above $LiNH_2$ is one of the products of hydrogenation of Li_3N, and NaOH is also a hydrogenated product of Na_2O [14]. The formation of these compounds upon hydrogenation of the unannealed material probably occurred, and the co-existence of these species along with other hydrogenated species such as LiH and NaH had an effect on their melting points. After annealing, the DSC results were quite similar to those for the annealed Li_2O-doped samples (cf. Fig. 3), inspite of the remarkable difference observed in the XRD patterns. Annealing resulted in a shift of the exothermic peak to higher temperature with a relatively narrower exotherm measured for the sample annealed at higher temperature (620 °C). An endothermic peak corresponding to the melting transition of $LiNH_2$ was also seen for both annealed samples.

Hydrogen absorption/desorption kinetics were measured for the doped material before and after annealing (Fig. 7). The unannealed sample absorbed 6.4 wt.% H at 240 °C. Meanwhile, doped Li_3N annealed at 400 °C absorbed 4.4 wt.% H at the same temperature. Both materials desorbed hydrogen partially. The difference in hydrogen uptake capacity between the unannealed and annealed sample can be explained at least in part by the presence of the unidentified phase in the latter. This unidentified phase did not seem to absorb any hydrogen and the lower hydrogen absorption was solely due to the presence of α-Li_3N in the sample, which is

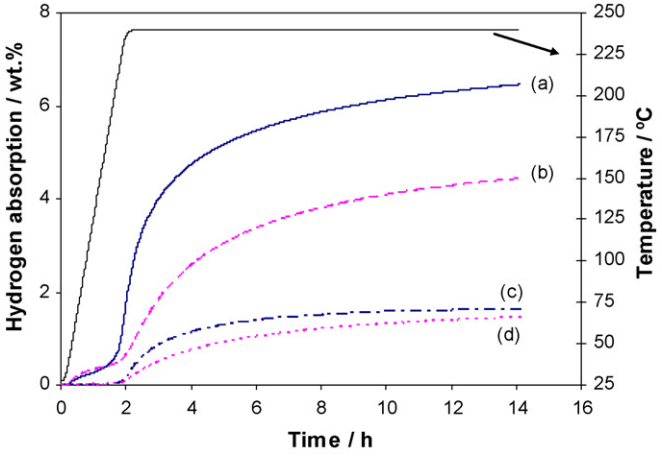

Fig. 7. Hydrogen absorption/desorption kinetic curves (room temperature to 240 °C) for 5 mol% Na_2O-doped Li_3N: (a) absorption for unannealed (milled) sample, (b) absorption for sample annealed at 400 °C, (c) desorption for unannealed (milled) sample, and (d) desorption for sample annealed at 400 °C.

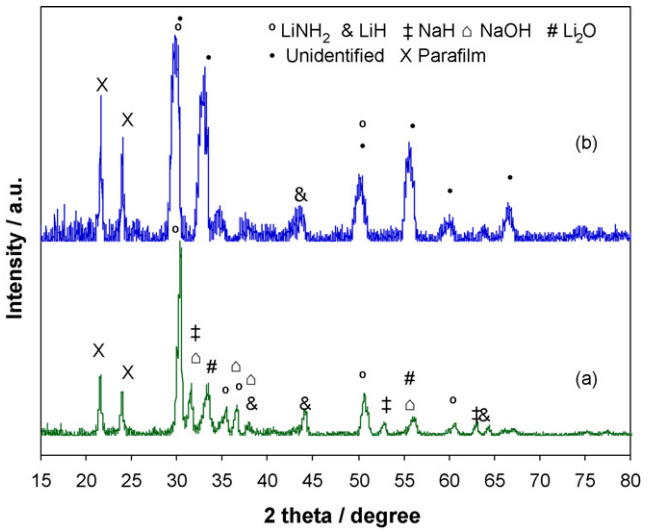

Fig. 8. XRD patterns after hydrogenation at 240 °C for 5 mol% Na_2O-doped Li_3N: (a) unannealed and (b) annealed at 400 °C.

confirmed by XRD (Fig. 8). Fig. 8 illustrates that for the unannealed sample, both Na_2O and Li_3N reacted with hydrogen to generate NaH along with NaOH, and $LiNH_2$ along with LiH, respectively. This is in agreement with the observation of two melting transitions for this material, which are assigned to NaOH and $LiNH_2$. Li_2O, which is unreactive to hydrogen, was also present. The hydrogen storage capacity measured for this material; however, is not high enough to match the complete conversion to its hydrogenated species. Therefore some unreacted material might still be present, although not visible in the XRD pattern. The presence of spectator Li_2O was also responsible for the lowered hydrogen capacity. Meanwhile, for the sample annealed at 400 °C, after hydrogenation, all the α-Li_3N reflections disappeared from the XRD pattern but the unidentified peaks persisted and diffraction peaks associated with LiH and presumably $LiNH_2$ emerged; we note here that there was an overlap of $LiNH_2$ peaks with some of the unidentified features in the XRD pattern. No evidence of the formation of NaH and/or NaOH was seen. The hydrogen absorption capacity of the sample annealed at 620 °C was even lower reaching only 1.8 wt.% at 345 °C. This is in accordance with the lower α-Li_3N content in the material as observed by XRD. Therefore, for both annealed samples the unidentified material that was present did not participate in the hydrogenation reaction; a behaviour that was also observed for Li_2O in the case of Li_2O-doped Li_3N.

4. Conclusions

The results of this study demonstrate that milling Li_3N without the addition of any dopant results in a lower onset temperature for hydrogenation and better hydrogen cycling properties than those of unmilled Li_3N. Addition of Li_2O, followed by milling and annealing, affects the onset temperature of hydrogenation as well as the cycling performance of Li_3N. Annealing at 400 °C leads to an improved cyclability over that of as-received Li_3N, but the results are very similar to those of the undoped milled sample. Thus, heat treatment at 400 °C is necessary for the hydrogen cycling performance of the Li_2O-doped sample to match that of milled Li_3N. This work has shown that doping Li_3N with Li_2O does not enhance the hydrogen storage performance of Li_3N: Li_3N and Li_2O exist as separate phases in the doped material with no compelling evidence of O^{2-} substitution of N^{3-}, and most likely no improved Li^+ and H^+ mobility. Doping of Li_3N with Na_2O followed by annealing results in the formation of an unidentified phase, which does not participate in the hydrogen storage reactions. Meanwhile, for unannealed Na_2O/Li_3N, both Na_2O and Li_3N react with hydrogen and contribute to the storage capacity of the system.

Acknowledgements

The authors would like to acknowledge Dr. Ven Reddy for carrying out some of the XRD measurements. This work was supported by the *Natural Sciences and Engineering Research Council* of Canada (NSERC), *Canada Foundation for Innovation* (CFI) and Hydrogen Storage Media (HSM) Systems Inc.

References

[1] US Department of Energy, Office of Basic Energy Sciences (2004) Basic Research Needs for the Hydrogen Economy. US DOE, Washington, DC, available at http://www.sc.doe.gov/bes/hydrogen.pdf.
[2] S. Orimo, Y. Nakamori, J.R. Eliseo, A. Züttel, C.M. Jensen, Chem. Rev. 107 (2007) 111–4132.
[3] P. Chen, Z. Xiong, J. Luo, J. Lin, K.L. Tan, Nature 420 (2002) 302–304.
[4] Y.H. Hu, N.Y. Yu, E. Ruckenstein, Ind. Eng. Chem. Res. 43 (2004) 4174–4177.
[5] Y.H. Hu, N.Y. Yu, E. Ruckenstein, Ind. Eng. Chem. Res. 44 (2005) 4304–4309.
[6] T. Ichikawa, N. Hanada, S. Isobe, H.Y. Leng, H. Fujii, J. Alloys Compd. 404–406 (2005) 435–438.
[7] T. Ichikawa, S. Isobe, N. Hanada, H. Fujii, J. Alloys Compd. 365 (2004) 271–276.
[8] S. Orimo, Y. Nakamori, G. Kitahara, K. Miwa, N. Ohba, T. Noritake, S. Towata, Appl. Phys. A 79 (2004) 1765–1767.
[9] W. Luo, J. Alloys Compd. 381 (2004) 284–287.
[10] A. Sudik, J. Yang, D. Halliday, C. Wolverton, J. Phys. Chem. C 111 (2007) 6568–6573.
[11] W. Luo, S. Sickafoose, J. Alloys Compd. 407 (2006) 274–281.
[12] P.A. Chater, P.A. Anderson, J.W. Prendergast, A. Walton, V.S.J. Mann, D. Book, W.I.F. David, S.R. Johnson, P.P. Edwards, J. Alloys Compd. 446–447 (2007) 350–354.
[13] Z. Xiong, G. Wu, J. Hu, Y. Liu, P. Chen, W. Luo, J. Wang, Adv. Funct. Mater. 17 (2007) 1137–1142.
[14] B.A. Boukamp, R.A. Huggins, Mater. Res. Bull. 13 (1978) 23–32.
[15] W.I.F. David, M.O. Jones, D.H. Gregory, C.M. Jewell, S.R. Johnson, A. Walton, P.P. Edwards, J. Am. Chem. Soc. 129 (2007) 1594–1601.
[16] Y.H. Hu, E. Ruckenstein, Ind. Eng. Chem. Res. 43 (2004) 2464–2467.
[17] A.R. West, Solid State Chemistry and Its Applications, John Wiley & Sons Ltd., Oxford, 1984.
[18] J. Wahl, Solid State Commun. 29 (1979) 458–490.
[19] Q. Xu, R. Wang, T. Kiyobayashi, N. Kuriyama, T. Kobayashi, J. Power Sources 155 (2006) 167–171.
[20] A. Huq, J.W. Richardson, E.R. Maxey, D.M. Chandra, W. Chien, J. Alloys Compd. 436 (2007) 256–260.
[21] W. Chien, J. Lamb, D. Chandra, A. Huq, J. Richardson Jr., E. Maxey, J. Alloys Compd. 446–447 (2007) 363–367.
[22] Z. Xiong, G. Wu, J. Hu, P. Chen, J. Power Sources 159 (2006) 167–170.